Perturbations of Functional Interactions with Myosin Induce Long-Range Allosteric and Cooperative Structural Changes in Actin†

Ewa Prochniewicz and David D. Thomas*

Department of Biochemistry, University of Minnesota Medical School, Minneapolis, Minnesota 55455

Received May 21, 1997; Revised Manuscript Received August 20, 1997⊗

ABSTRACT: The role of the rotational dynamics of actin filaments in their interaction with myosin was studied by comparing the effect of myosin subfragment 1 (S1) with two other structural perturbations, which have substantial inhibitory effects on activation of myosin ATPase and *in vitro* motility of F-actin: (1) binding of the antibody fragment $F_{ab}(1-7)$ against the first seven N-terminal residues and (2) copolymerization with monomers treated with the zero-length cross-linker 1-ethyl-3-[3-(dimethylamino)propyl]carbodiimide (EDC), referred to as EDC-actin. The rotational motion of actin was measured by time-resolved phosphorescence anisotropy (TPA) of erythrosin iodoacetamide (ErIA) attached to Cys 374 on actin. The binding of S1 in a rigor complex (no nucleotide) induced intramonomer (allosteric) and intermonomer (cooperative) structural changes that increased the residual anisotropy of labeled F-actin, indicating a conformational change in the region of the C terminus. Similar allosteric and cooperative changes were induced by binding of $F_{ab}(1-7)$ and by copolymerization of the ErIA-labeled actin monomers with EDC-actin. This suggests that the functional perturbations transform actin to a form resembling the rigor actomyosin complex. The correlation of the perturbation-induced changes in TPA of actin with the functional effects suggests that the actomyosin interaction can be inhibited by stabilization of actin in one of its structural intermediates.

Interaction of actin with myosin in the presence of adenosine 5′-triphosphate (ATP[1]) results in activation of myosin ATPase and sliding movement along myosin heads. The two basic functions of actin can be substantially affected by site-directed perturbations such as mutations in subdomain 1 of actin (*1*−*5*) and proteolytic cleavage of the DNase loop in subdomain 2 (*6*). These functional effects directly indicate that the molecular mechanism of motility depends on the structural properties of actin and its complex with myosin.

Substantial effects of myosin on the structure and dynamics of actin have been observed using spectroscopy and microscopy. Fluorescence studies established that in the absence of ATP (rigor), binding of myosin changes the signal from actin-bound labels, interpreted as changes in the local environment of the probe or increased filament flexibility (*7*−*10*). Increased flexibility has been also observed using electron microscopy (*11*). Optical microscopy directly confirmed that binding of HMM increases the millisecond bending flexibility of actin filaments and revealed that this effect becomes more pronounced in the presence of ATP (*12*). However, ST-EPR of actin spin-labeled at Cys 374 showed that rigor binding of myosin restricts microsecond rotational motions in actin (*13*, *14*); in this case no difference between the effect of myosin bound in the absence of ATP and that of myosin bound in the presence of ATP was observed (*15*).

In the present work we examine the effect of myosin binding on microsecond actin dynamics using time-resolved phosphorescence anisotropy (TPA) of erythrosin iodoacetamide labeled actin. This method has been previously applied to characterize the dynamics of actin filaments alone (*16*): the analysis of data in terms of several models of rotational motions allowed determination of F-actin's torsional flexibility and the orientation of the dye-binding region (*16*, *17*). We also assess the functional role of the microsecond time scale motions in actin and its complex with myosin by applying structural perturbations to actin that are known to affect the interactions with myosin.

The first perturbation was binding of the antibody fragment $F_{ab}(1-7)$ against the first seven N-terminal residues of actin. F_{ab} binds to actin and acto-S1, but in the presence of ATP this F_{ab} affected the binding of S1, a catalytic step in the ATP hydrolysis by actomyosin and development of active tension in muscle fibers (*18*−*20*), indicating that at least some of the residues 1−7 may be involved in interactions with myosin. This is supported by a model of the acto-S1 complex, which shows contact between the first four N-terminal residues of actin and the catalytically important loop 626−647 of myosin (*21*).

The second perturbation was copolymerization of ErIA-labeled monomers with unlabeled, EDC-treated monomers, referred to as EDC-actin (*22*−*24*). Filaments polymerized from EDC-actin do form a rigor complex but do not bind to myosin in the presence of ATP and are not motile in the *in vitro* motility assay. This inhibitory effect appears also in filaments obtained by copolymerization of the EDC-actin

† This work was supported by a grant to E.P. from the American Heart Association, Minnesota Affiliate, and by a grant to D.D.T. from NIH (AR32961).

* Author to whom correspondence should be addressed. [telephone (612) 625-0957; fax (612) 624-0632; e-mail ddt@ddt.biochem.umn.edu].

⊗ Abstract published in *Advance ACS Abstracts,* October 1, 1997.

[1] Abbreviations: ATP, adenosine 5′-triphosphate; ErIA, erythrosin iodoacetamide; EDC, 1-ethyl-3-[3-(dimethylamino)propyl]carbodiimide; TPA, transient phosphorescence anisotropy; S1, myosin subfragment 1; $F_{ab}(1-7)$, affinity-purified F_{ab} fragment of polyclonal peptide antibodies raised against the first seven N-terminal residues of α-skeletal actin; SDS−PAGE, sodium dodecylsulfate−polyacrylamide gel electrophoresis.

S0006-2960(97)01201-4 CCC: $14.00

with untreated monomers, suggesting functionally important cooperative (intermonomer) interactions within the actin filament (*22*−*24*). Thus, the functional effects of copolymerization are qualitatively similar to the effect of F_{ab}, and we have performed TPA studies to determine whether the two perturbations have also some common structural effects. The experiments using the copolymers have an additional advantage: localization of the ErIA label on the untreated monomers allows direct detection of the transfer of changes from the unlabeled EDC-actin, thus providing direct detection of intermonomer cooperativity in the actin filament.

The results are discussed in terms of allosteric (intramonomer) and cooperative (intermonomer) changes in actin structure and their possible role in functional interactions with myosin.

MATERIALS AND METHODS

Sample Preparation. Actin was prepared and labeled with the phosphorescent dye ErIA as described previously (*16*, *17*). Myosin subfragment 1 (S1) was obtained by α-chymotryptic digestion of myosin from rabbit skeletal muscle (*25*). The F_{ab} fragment of polyclonal peptide antibodies raised against the first seven N-terminal residues of α-skeletal actin [$F_{ab}(1-7)$] and column purified (*18*) was a gift from Dr. E. Reisler.

To prepare EDC-actin, monomeric actin (0.5 mg/mL) in 5 mM Hepes (pH 7.0), 0.3 mM ATP, and 0.1 mM $CaCl_2$ was incubated for 30 min at 25 °C with freshly dissolved 15 mM EDC (*22*); the reaction was stopped with 1% β-mercaptoethanol. EDC-actin was dialyzed into G-buffer (5 mM Tris, pH 8.0, 0.2 mM ATP, 0.1 mM $CaCl_2$) and ultracentrifuged (30 min at 200000*g*) to remove any aggregates: on SDS−PAGE only one band corresponding to a monomer was observed (*22*).

Monomeric ErIA-labeled actin and EDC-actin (0.5 mg/mL) were mixed at various ratios in G-buffer and copolymerized by the addition of 0.1 M KCl followed by 1 h of incubation at 25 °C. The copolymers, as well as control ErIA-F-actin, were ultracentrifuged (1 h at 200000*g*); pellets were suspended in F-buffer (50 mM KCl, 20 mM Tris, pH 8.0, 0.1 mM $CaCl_2$) containing 0.2 mM ATP and clarified by 10 min of centrifugation at 21000*g*. The composition of copolymers was obtained by calculating first the fraction of ErIA-labeled monomers in the filaments as the ratio of the absorbance at 543 nm (absorption peak of ErIA-actin) per milligram of protein in the copolymer relative to that in the control ErIA-F-actin; the fraction of EDC-actin was obtained as the difference: (1 − ErIA-actin)/total actin. Before any physical or functional measurement, each actin sample was stabilized by a 1:1 molar ratio of phalloidin to actin, to ensure that the fraction of monomeric actin was negligible even at very low protein concentrations.

Protein Concentration. The concentration of unlabeled proteins was measured by ultraviolet absorption, assuming molar extinction coefficients of 0.63 mg mL^{-1} cm^{-1} for actin at 290 nm and 0.75 mg mL^{-1} cm^{-1} for S1 at 280 nm. The concentration of ErIA-labeled actin and EDC-actin was measured using the Bradford protein assay (*26*) using unmodified actin as a standard.

Light Scattering Measurements. Light scattering was measured at 23 °C in a SPEX Fluorolog fluorometer, with the excitation and emission monochromators set at 400 nm. Light scattering intensities are expressed in arbitrary units.

Spectroscopic Experiments. For TPA experiments, phalloidin-stabilized F-actin in F-buffer plus 0.2 mM ATP was diluted in F-buffer to 0.06 mg/mL (unless stated otherwise). Complexes of actin with S1 were preincubated at room temperature for 20 min to 1 h to complete the hydrolysis of all ATP remaining in the actin sample, as determined from changes in light scattering intensity after addition of S1 to actin. Before TPA measurement, oxygen was removed by incubation with glucose oxidase (220 μg/mL), catalase (36 μg/mL), and glucose (45 μg/mL) (*27*).

TPA was measured as described previously (*16*, *17*, *28*). The actin-bound dye (ErIA) was excited with a 10-ns pulse of vertically polarized light at 540 nm, followed by detection of the time-dependent phosphorescence emission with a time resolution of 50 ns/channel. Phosphorescence signals were digitized with a transient recorder (dwell time ≥ 50 ns/channel resolution), and repeated transients were averaged by the microcomputer. The time-resolved phosphorescence anisotropy was calculated as

$$r(t) = \frac{I_{vv}(t) - GI_{vh}(t)}{I_{vv}(t) + 2GI_{vh}(t)} \tag{1}$$

where $I_{vv}(t)$ and $I_{vh}(t)$ are the vertically and horizontally polarized components of the emission signal. G is an instrumental correction factor, determined by performing the experiment with a solution of ErIA-labeled bovine serum albumin in 98% glycerol and adjusting G to give a residual anisotropy value of zero, the theoretical value for an isotropically tumbling chromophore.

Anisotropy Data Analysis: Model-Independent Fit to the Sum of Exponentials. The initial anisotropy $r_0 = r(t = 0)$, rotational correlation times ϕ_i, amplitudes $A_i = r_i/r_0$, and the final anisotropy r_∞ were determined by fitting the anisotropy to a sum of n exponential terms and a constant:

$$r(t) = \sum_{i=1}^{n} r_i \, e^{-t/\phi_i} + r_\infty \tag{2}$$

The data were fitted in the 3−500 μs time range. The fit was judged to be optimal for a particular value of n if decreasing n made the fit worse and increasing n failed to improve it, as judged from the residuals (data minus fit) and χ^2. For the currently used samples the fit was optimal for $n = 2$, with the residual never exceeding 1.5% of the maximum anisotropy. The fitted final anisotropy r_∞ was within 10% of the calculated average $r(t)$ in the 400−500 μs time range, indicating that the decay reached a plateau level within the analyzed time window. The observed initial anisotropy r_0, as fit to eq 2, is lower than the theoretical maximum value by an amplitude reduction factor $\kappa \leq 1$ due to motions on the time scale too fast to be detected (*16*).

For rotational motions involving isotropic wobble of the observed transition dipole of the probe in a cone, the half-angle of the cone θ_c is given by (*29*)

$$r_\infty/r_0 = \left[\frac{1}{2}\cos\theta_c(1 + \cos\theta_c)\right]^2 \tag{3}$$

Anisotropy Data Analysis: Model of a Segmented Flexible Cylinder. Anisotropy decays were analyzed in terms of a

model that describes the rotational diffusion of a segmented flexible filament with mean local cylindrical symmetry (*30*). We have shown previously (*16*) that when the contribution from rigid body rotations can be neglected, the anisotropy decay of actin filaments is described by the formula (*30*)

$$r(t) = \kappa\left[A_0 + A_1 \exp\left(-\frac{1}{4}\sqrt{\frac{t}{\Phi}}\right) + A_2 \exp\left(-\sqrt{\frac{t}{\Phi}}\right)\right] \quad (4)$$

The amplitudes A_i are functions of the orientation of the absorption and emission dipoles of the bound dye relative to the filament axes, θ_a and θ_e, as described previously (*16, 30*):

$$A_0 = \frac{1}{10}(3\cos^2\theta_a - 1)(3\cos^2\theta_e - 1) \quad (5)$$

$$A_1 = \frac{6}{5}\sin\theta_a \cos\theta_a \cos\Psi_{ea} \sin\theta_e \cos\theta_e \quad (6)$$

$$A_2 = \frac{3}{10}\sin^2\theta_a \cos 2\Psi_{ea} \sin^2\theta_e \quad (7)$$

The time constant Φ (eq 4) is proportional to the square of the filament radius a and the torsional rigidity C

$$\Phi = (\pi a)^2 C\eta/4(k_B T)^2 \quad (8)$$

where η is the solvent viscosity. The torsional rigidity C (dyn × cm^2) is the torque in dyn × cm required to twist a 1-cm filament by 1 radian.

Alternatively, if the filaments are completely rigid ($C = \infty$), the anisotropy decay due to rigid-body rotations is described by

$$r_i(t) = \kappa[A_0 \exp(-t6D_{i\perp}) + A_1 \exp[-t(D_{i\parallel} + 5D_{i\perp})] + A_2 \exp[-t(4D_{i\parallel} + 2D_{i\perp})]] \quad (9)$$

where $D_{i\parallel}$ and $D_{i\perp}$ are the diffusion coefficients around long (z) and short (x) axes of the filament, respectively. For actin filaments having a broad length distribution, the observed anisotropy is the sum of the contributions from filaments within each particular length group l_i, weighted by the fraction of labeled protomers in the filaments belonging to the group

$$r(t) = \sum_{i=1}^{n} r_i(t)\beta_i \qquad \beta_i = k_i l_i / \sum_{i=1}^{n} k_i l_i \quad (10)$$

where k_i is the number of filaments with a length l_i. The distribution of filament lengths, l_i, was determined from electron microscopy (*16*).

The anisotropy decays were fitted to eqs 2, 4, and 10 using a microcomputer. Results are given below as mean ± SEM with indicated number of measurements n.

Reagents. The phosphorescent dye ErIA was purchased from Molecular Probes (Eugene, OR) and stored at −20 °C. ATP, EDC, and phalloidin were obtained from Sigma (St. Louis, MO). All other chemicals were of reagent grade.

RESULTS

Effect of Rigor Binding of S1 on TPA of ErIA-F-Actin. Binding S1 to ErIA-F-actin, in the absence of ATP, resulted in substantial changes in the phosphorescence anisotropy decay, with most of the effect complete at a molar ratio of S1 to actin of 0.4−0.6 (Figure 1). The principal effect of S1 binding appears to be an increase in the final anisotropy r_∞, i.e., a decrease in the amplitude of anisotropy decay. This was confirmed by the fit to a sum of two exponential terms and a constant (eq 2), which shows that at [S1]/[A] = 1, S1 binding increases the normalized final anisotropy $A_\infty = r_\infty/r_0$ up to (2.24 ± 0.06)-fold ($n = 6$). The increase in A_∞ was accompanied by an increase in the correlation times ϕ_i of the rotational motions in actin: up to (1.25 ± 0.07)-fold ($n = 13$) for ϕ_1 and up to (1.83 ± 0.13)-fold ($n = 13$) for ϕ_2.

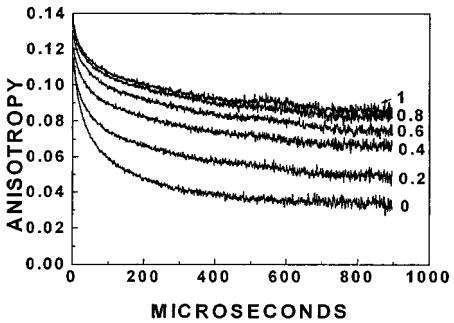

FIGURE 1: Effect of S1 binding on TPA of ErIA-F-actin. ErIA-F-actin (0.06 mg/mL in F-buffer + 1 mM $MgCl_2$) was preincubated with various concentrations of S1 for 15−30 min at room temperature, and then TPA was measured at 25 °C. The molar ratio of S1 to actin is indicated.

We assessed our results further by restricting the fits to eq 2, assuming either that (a) S1 binding changes only the amplitudes A_i without affecting the correlation times ϕ_i, or (b) S1 binding changes only the correlation times ϕ_i without affecting the amplitudes A_i. Both models led to lower quality fits (not shown), confirming that the changes in TPA reflect changes in both amplitudes and correlation times of rotational motions.

One possible explanation for increased anisotropy is immobilization of acto-S1 filaments by bundling (*31*), but the electron microscope observation of samples prepared for TPA revealed only single acto-S1 filaments, similar to the filaments of F-actin alone, but no bundles. The possibility of bundling was further examined by the measurement of light scattering. The light scattering intensity of acto-S1 filaments is proportional to the fraction of the sites occupied by S1 and remains constant in time (*32*), while its time-dependent increase has been associated with appearance of thick bundles, seen by electron microscopy (*31*). The data in Figure 2A show that under conditions of our TPA experiments the association of added S1 with ErIA-F-actin increased the light scattering intensity to a value constant in time; this result was obtained in the range of molar ratio of S1 to actin from 0.2 to 1.5, indicating that the acto-S1 filaments do not form bundles. On the other hand, a control experiment (Figure 2B) confirmed that when acto-S1 filaments were incubated under conditions which promote bundling (0.15 M KCl, 20 mM Hepes, pH 7.0, 2 mM $MgCl_2$, 1 mM $NaHPO_4$), the light scattering intensity gradually increased, consistently with the previously reported data (*31*). We conclude that our choice of buffer conditions effectively prevented bundling of actin filaments by S1.

TPA of acto-S1 was independent of actin concentration in the range from 0.01 to 1 mg/mL, indicating that increasing

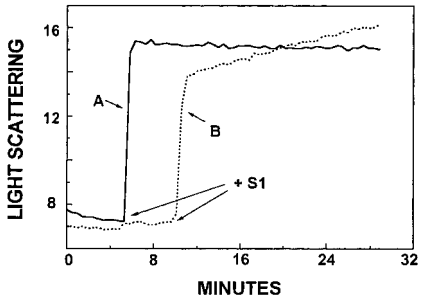

FIGURE 2: Light scattering intensity of acto-S1 ([S1]/[A] = 0.2) during incubation at room temperature in (A) F-buffer + 1 mM $MgCl_2$ and (B) 0.15 M KCl, 20 mM Hepes, pH 7.0, 2 mM $MgCl_2$, 1 mM $NaHPO_4$. Actin concentration was 0.3 mg/mL. The arrows indicate addition of S1 to ErIA-F-actin.

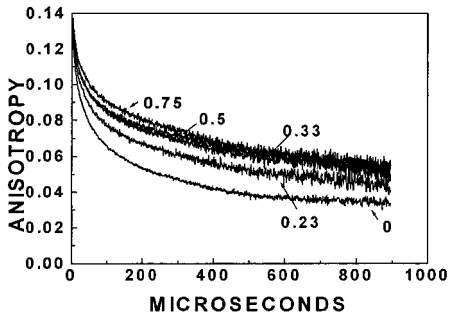

FIGURE 3: Effect of F_{ab}(1−7) binding on TPA of ErIA-F-actin. ErIA-F-actin (0.06 mg/mL in F-buffer + 1 mM $MgCl_2$) was preincubated with various concentrations of F_{ab} for about 30 min at 25 °C and then TPA was measured. The ratio of bound F_{ab} to actin, indicated in the figure, was calculated by assuming a binding constant of 7×10^5 M^{-1} (*18*).

Table 1: Effect of Actin Perturbations on the Angular Amplitude (θ_c) of the Wobbling Motions of Cys 374-bound ErIA[a]

filament	A_∞	cone angle θ_c (deg)
F-actin	0.291 ± 0.004 (n = 6)	49.29 ± 0.24
acto-S1	0.651 ± 0.022 (n = 6)	30.05 ± 1.13
actin + F_{ab}	0.433 ± 0.029 (n = 4)	41.31 ± 1.55
copolymer	0.651 ± 0.022 (n = 4)	28.02 ± 1.00

[a] Tha data are shown as mean ± SEM for acto-S1 at [S1]/[A] = 1, for actin + F_{ab} at [F_{ab}]/[A] = 0.75, and for copolymers with fraction of EDC-actin ranging from 0.61 to 0.69.

entanglement of long filaments in solution (*16*) does not affect S1-induced changes in the dynamics of F-actin.

Effect of F_{ab}(1−7) on TPA of Actin. As in the case of S1 (Figure 1), binding of F_{ab} increased the normalized final anisotropy A_∞ and correlation times, with the effect saturating at substoichiometric levels of F_{ab} (Figure 3). However, the maximum effect for F_{ab} was less than for S1: the maximum increase in A_∞ was (1.53 ± 0.04)-fold (n = 4) (Table 1), and the corresponding increases in the correlation times ϕ_i were (1.08 ± 0.04)-fold (n = 4) for ϕ_1 and (1.38 ± 0.11)-fold (n = 4) for ϕ_2.

Effect of Copolymerization of EDC-Actin with ErIA-Labeled Monomers on TPA. Previously, the observation of copolymers of unmodified actin and rhodamine-labeled EDC-actin under a fluorescence microscope revealed filaments of similar and homogeneously distributed brightness, indicating random copolymerization (*22*). The presence of unlabeled EDC-actin in the filaments with the ErIA label on the untreated monomers had a substantial effect on TPA (Figure 4). A_∞, obtained from the fits of TPA of the copolymers to the sum of two exponential terms (eq 2), increased (2.21 ± 0.09)-fold (n = 4). The maximum value of A_∞ is remarkably similar to that obtained for acto-S1 (Table 1). However, in contrast to the effect of S1 and F_{ab}, the correlation times ϕ_1 and ϕ_2 decreased to 0.61 ± 0.15 (n = 3) and 0.49 ± 0.14 (n = 3), respectively, of the values obtained for F-actin.

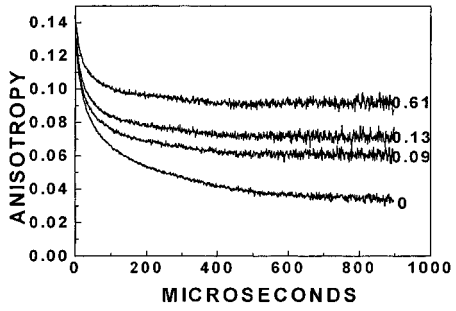

FIGURE 4: Effect of copolymerization of EDC-actin with ErIA-labeled monomers on TPA. Actin concentration was 0.06 mg/mL, F-buffer + 1 mM $MgCl_2$, 25 °C. The fraction of EDC-actin in the filaments is indicated.

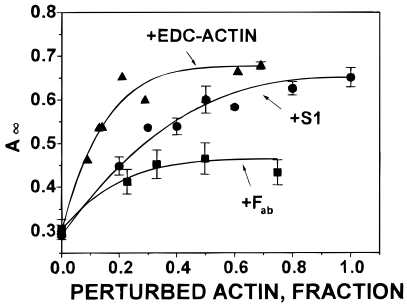

FIGURE 5: Analysis of the effects of actin perturbations on normalized final anisotropy (A_∞) in terms of the linear lattice model (*33*). The data were fitted to the equation $A_\infty = A_{max} - (A_{max} - A_{F-actin})(1 - x)^N$, where A_{max} is the maximum value of A_∞, obtained at [S1]/[A] = 1, [F_{ab}]/[A] = 0.5, and fraction of EDC-actin in copolymers = 0.69; $A_{F-actin}$ is the A_∞ of unperturbed F-actin; x is the fraction of perturbed monomers in the filament; and N is the number of monomers affected by perturbation. The curves correspond to the best fit with N = 2.6 ± 0.2 (acto-S1, ●), 4.9 ± 1.1 (actin + F_{ab}, ■), and 6.7 ± 0.9 (copolymers, ▲).

The possibility of filament bundling has been eliminated by observation of phalloidin−rhodamine-labeled copolymers under the fluorescence microscope: in the range of protein concentration from 0.005 to 0.06 mg/mL, only single filaments were seen. The effect of copolymerization on TPA also could not be due to the decreasing fraction of labeled monomers in the filament and increasing noise in the data, since copolymerization of similar amounts of unlabeled and unmodified actin with ErIA-labeled monomers had no effect on the decay. Entanglement of the copolymers in solution did not have any effect on the dynamics of the filaments, since a 16-fold increase in the protein concentration, from 0.03 to 0.5 mg/mL, had no significant effect on TPA.

Analysis of Cooperativity Using a Linear Lattice Model. The increase in A_∞ with increasing fraction of perturbed actin monomers in the filament was analyzed in terms of a linear lattice model (*33*), assuming that perturbation of one monomer in an actin filament affects a segment containing N monomers (Figure 5). In all cases a satisfactory fit required $N > 1$, indicating cooperativity of changes, with N ranging from 2.6 ± 0.2 (+S1) to 4.9 ± 1.1 (+F_{ab}) to 6.7 ± 0.9 (+EDC-actin).

To assess the functional significance of the observed spectroscopic changes, we compared directly the copolym-

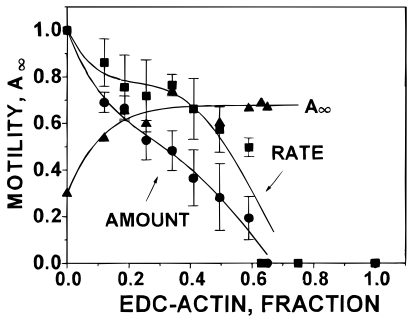

FIGURE 6: Comparison of effect of copolymerization of EDC-actin and untreated monomers on A_∞ with the effect on the *in vitro* motility of actin filaments. A_∞ of copolymers (▲) as in Figure 5, the motility data were obtained previously (*16*). The sliding rate (■) and the number of sliding filaments (●) are expressed as a fraction of values measured for the unmodified actin filaments in the same experiment. The motility assay was done on a surface saturated with HMM in 2.5 mM $MgCl_2$, 10 mM Tris, pH 8.0, 0.2 mM ATP, 1% β-mercaptoethanol, and oxygen removing enzymes, at 25 °C.

erization-induced changes in A_∞ with the changes in motility of the copolymers in the *in vitro* motility assay, which were reported previously (*23*). As shown in Figure 6, both spectral and functional changes occurred in a similar range of the fraction of EDC-actin in the filaments. On the other hand, the increase in A_∞ reached a maximum before complete inhibition of movement, indicating that the correlation between spectroscopic and functional data is not a simple one. This could be due to different sensitivities of these two measurements to the structural changes in actin: in the high-density HMM motility assay, a small number of unmodified actin monomers could still be capable of generating movement (*34*), but their contribution to the phosphorescence intensity would be too small to affect the TPA decay. Another possibility is that our TPA measurements do not detect all of the structural changes that affect the mechanism of motility.

Modeling the Molecular Dynamics. The analysis of changes in A_∞ in terms of the wobble-in-cone model (eq 3) shows that all perturbations decrease the cone angle θ_c, i.e., decrease the amplitude of the wobbling motions: S1 binding and copolymerization with EDC-actin decrease θ_c by about 20° and F_{ab} binding decrease θ_c by about 10° (Table 1).

We have shown previously that the rigid body rotation model (eq 10) cannot explain TPA of actin filaments alone (*16*), and Figure 7A (plot RBR) shows that this model also produces a very poor fit for the complex of actin with S1. In this analysis we assumed that S1 binding increased the diameter of the filaments from 45 to 130 Å, as estimated from the electron micrographs of negatively stained acto-S1 filaments (*35*), without effect on their length and the orientation of the transition dipoles of the bound ErIA. The quality of the fit remained low when changes were allowed in both the radius and the orientation of the dipoles (not shown). A similarly bad fit was obtained for the complex of actin with F_{ab} ([Fab]/[A] = 0.75) or copolymers. Although the filament length of copolymers (fraction of EDC-actin ranging from 0.50 to 0.60) was shortened from L_n = 4.2 μm (*16*) to about 1 μm, the residuals of the fit ranged from 17% to 40% of the anisotropy values (data not shown) even if all fit parameters were freely adjustable, indicating that the TPA data cannot be described by the rigid body rotation model.

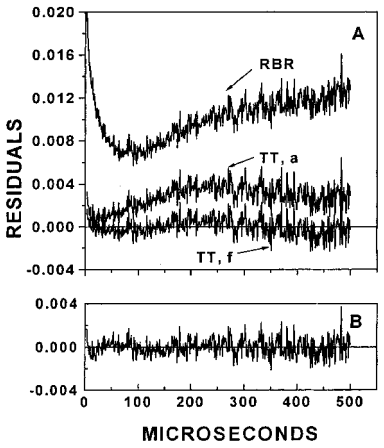

FIGURE 7: Residuals of TPA fits of acto-S1 ([S1]/[A] = 1) to the models of rotational motions. (A) Plot RBR, the rigid body rotation model (eq 10) with the diameter of the filament set at 130 Å; plots TT,a and TT,f, the torsional twist model (eq 4). In plots RBR and TT,f all fit parameters were adjustable, while in plot TT,a the orientation of the absorption dipole of the actin-bound ErIA was fixed at $\theta_a = 30.2 \pm 2.5°$(*16*) and all other parameters were adjustable. (B) Fit to the sum of two exponential terms (eq 2), which gives A_∞ in the wobble-in-cone model (eq 3).

Table 2: Effect of Actin Perturbations on the Orientation of the Transition Dipoles of ErIA (θ_a and θ_e) and the Time Constant Φ

filament	Φ (μs)	θ_a (deg)	θ_e (deg)
F-actin	3.66 ± 0.1 ($n = 5$)	27.68 ± 0.00	47.79 ± 0.16
acto-S1	14.64 ± 3.00 ($n = 7$)	7.75 ± 0.88	43.66 ± 0.54
actin + F_{ab}	7.44 ± 0.28 ($n = 3$)	11.75 ± 0.06	46.52 ± 0.06
copolymer	1.14 ± 0.13 ($n = 6$)	9.64 ± 2.37	41.75 ± 0.57

[a] TPA of F-actin was fitted to the torsional twist model assuming $\theta_a = 30.2 \pm 2.5°$, as determined in TAA experiment (*16*); TPA of acto-S1, actin + F_{ab}, and copolymer were fitted with Φ, θ_a, θ_e, and κ adjustable. Tha data are shown as mean ± SEM for acto-S1 at [S1]/[A] = 1, for actin + F_{ab} at [F_{ab}]/[A] = 0.75, and for copolymers with fraction of EDC-actin ranging from 0.61 to 0.69.

On the other hand, TPA of the perturbed actins, as that of actin alone, was successfully fitted to the torsional twist model (eq 4), providing that all fit parameters were freely adjustable; the residuals of the fit obtained for acto-S1 ([S1]/[A] = 1) are shown in Figure 7A (plot TT,f). The quality of the fit to this model is comparable to that of the two-exponential fit (eq 2, Figure 7B), which represents the wobble-in-cone model. This analysis (Table 2) shows that the perturbations had diverse effects on the time constant Φ (eq 4), resulting in its increase as well as decrease. On the other hand, all perturbations changed the orientation of the dye (θ_a, θ_e) to a similar extent, suggesting that similar structural changes were induced in actin. Lower quality fits were obtained when it was assumed either that S1 binding does not change the time constant Φ (not shown) or that it does not change the orientation of the absorption dipole θ_a (Figure 7A, plot TT,a).

Thus, the results of analyses in terms of the wobble-in-cone and torsional twist model suggest that binding of F_{ab} and copolymerization may at least partially mimic the changes induced by S1. To assess this possibility, we examined the effect of S1 on TPA of the complex of actin with F_{ab} and of the copolymers.

Effect of Rigor Binding of S1 on TPA of the Complex of Actin with F_{ab}. The addition of S1 to the complex of actin and F_{ab} resulted in a further increase of final anisotropy, in

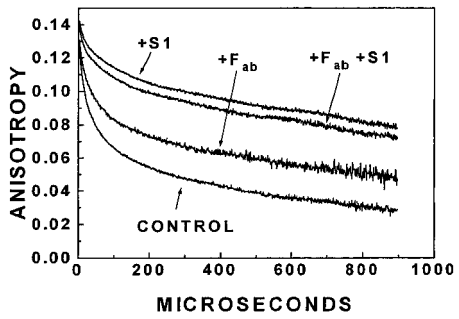

FIGURE 8: Effect of S1 binding to the complex of actin with F_{ab}-(1−7) on TPA. ErIA-F-actin (control, 0.06 mg/mL in F-buffer + 1 mM $MgCl_2$) was preincubated with F_{ab} ($[F_{ab}]/[A] = 0.5$) for about 30 min at 25 °C (+F_{ab}), and then S1 was added to the complex (+F_{ab} +S1) and to ErIA-F-actin alone (+S1) at a 1:1 molar ratio and TPA was measured (25 °C) after another 20 min of incubation.

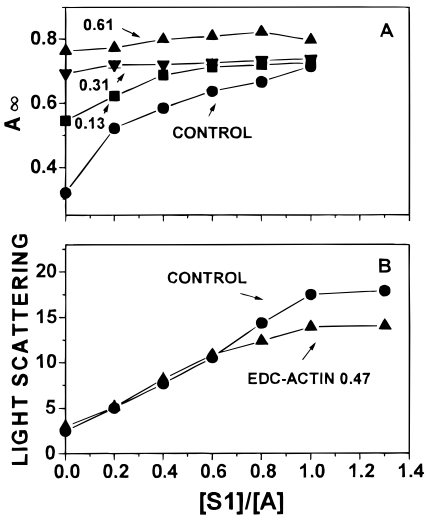

FIGURE 9: Binding of S1 to copolymers. (A) Effect of S1 on A_∞ of copolymers, the fraction of EDC-actin: 0, ● (control F-actin); 0.13, ■; 0.31, ▼ 0.61, ▲ The copolymers (0.06 mg/ml in F-buffer + 1 mM $MgCl_2$) were preincubated with various concentrations of S1 for 0.5−1 h at room temperature, and then TPA was measured at 25 °C. (B) Effect of S1 on the light scattering intensity of ErIA-F-actin (●) and copolymer, the fraction of EDC-actin = 0.47 (▲). The light scattering intensity was measured in the same conditions as TPA.

such a manner that the total effect of S1 and F_{ab} was similar to that of S1 alone (Figure 8). The order of addition of F_{ab} and S1 had no effect on the data. Thus, the effects of S1 and F_{ab} are not additive, suggesting that the bound F_{ab} at least partially mimics the effect of S1. This conclusion is supported by biochemical and structural data showing that F_{ab}-binding residues overlap with a fraction of the myosin-binding sites in the N terminus, and both F_{ab} and S1 can bind to the same monomers in an actin filament (*18*, *19*, *21*).

Effect of Rigor Binding of S1 on TPA of Copolymers. Addition of S1 to the copolymers induced changes in TPA that were qualitatively similar to the effects of S1 on unmodified actin, including the increase in the normalized final anisotropy (Figure 9A). However, the incremental effect of S1 decreased with increasing fraction of EDC-actin in the filament, so that the combined effect at saturating S1 levels was only slightly greater than the maximum effect for either S1 or EDC-actin alone. This result was independent of the protein concentration, in the range from 0.005 to 0.3 mg/mL.

The effect of S1 on the light scattering intensity of actin filaments was very similar for copolymers and control F-actin, showing that copolymerization did not inhibit binding of S1 to the filaments. Ultracentrifugation of the rigor complex confirmed this result, showing that at [S1]/[A] between 0.8 and 1, >95% of S1 is bound to F-actin, while ∼70% is bound to the copolymer. Thus, copolymerization slightly decreases the affinity of S1 for actin, but 70% of bound S1 is still more than sufficient to saturate the effect on A_∞ (Figures 1 and 5). Therefore, the nonadditive effect of copolymerization and S1 binding (Figure 9A) cannot be due to inhibition of S1 binding. It indicates that EDC-actin induces structural changes within the copolymers that mimic the effect of S1.

DISCUSSION

Intramonomer Allosteric Changes. Binding of S1 to F-actin and perturbation of its structure by F_{ab} and copolymerization with EDC-actin substantially increased the normalized final anisotropy A_∞ of the TPA, detected at Cys 374 (Figures 1, 3, and 5). The localization of the F_{ab} binding site within the first seven residues at the N terminus, about 20−30 Å distant from Cys 374, suggests that the effect is allosterically transferred between the two sites. Direct interaction of the F_{ab} molecule with the ErIA label seems unlikely, since fluorescence quenching revealed no effect of F_{ab} on the accessibility of a similar dye, fluorescein iodoacetamide, also bound to Cys 374 (*36*). Since the binding site of F_{ab} includes four charged residues at the N terminus that probably form electrostatic contacts with myosin (*21*), the changes induced by F_{ab} could represent at least a fraction of the changes induced by S1; this possibility is supported by the nonadditive effects of S1 and F_{ab} on TPA (Figure 8). The significantly larger effect of S1 than that of F_{ab} on A_∞ (Figures 5 and 8) indicates contributions from interactions with other sites in actin, which are proposed to be located in other regions of the N terminus (residues 24−25 and 91−100) and in subdomains 2 and 3 (*21*). Since the proposed crystal structure of the acto-S1 complex does not indicate direct contact between the heavy chain and Cys 374 (*21*), the effect of interaction with these sites seems to be mainly allosteric. The possibility of direct interaction of the A1 essential light chain of S1 with Cys 374 has been indicated by cross-linking and NMR studies (*37*, *38*), but studies on the solvent accessibility of fluorescent probes attached to Cys 374 did not detect a significant effect of S1 (*36*). The proposed allosteric effect of S1 is not limited to the C terminus of actin; it has also been proposed to explain changes in the region around Gln 41 (*39*) and the 61−69 sequence in subdomain 2 (*40*). These results, together with reported changes in the intramonomer distances upon binding of S1 (*41*), indicate that the effect of S1 is not limited to specific regions of the actomyosin interface but extends over a wider area of the actin monomer. These allosteric effects appear to be part of a network of structural pathways within the actin monomer, suggested by the reported coupling of conformational changes in the C terminus to changes in subdomain 2 and the nucleotide binding site (*36*, *42*−*45*).

Intermonomer Cooperativity. The analysis of changes in A_∞ show that each perturbation affects several monomers in an actin filament (Figure 5, $N > 1$), indicating intermonomer cooperativity. The effect of one bound S1 on two to three monomers (Figure 5) could be explained by a direct

interaction with two adjacent monomers, indicated by the cross-linking and structural data (*21, 46*) or by intermonomer cooperativity, where changes induced in a directly interacting monomer are transferred to the neighboring one. This cooperativity of changes in TPA is consistent with previously reported nonlinear changes in the spectral properties of actin labeled at Cys 374 by fluorescent, spin, and phosphorescent labels (*10, 13, 14, 47, 48*), which indicated that one bound myosin head can affect 2−25 monomers. Remarkable cooperativity has been seen in negatively stained filaments, even when HMM was present at extremely low molar ratios (1:200 or 1:300) with respect to actin (*49*). On the other hand, measurements of fluorescence from actin-bound ϵADP are inconsistent, showing both cooperative (*50*) and noncooperative response (*51*). A consistently noncooperative response was reported for pyrene-labeled actin (*9, 52, 53*). This diversity of conclusions could be caused by differences in the methods of measurement, different sensitivities of probes to structural changes in actin, probe-induced alterations of actin, and possible bundling of the acto-S1 filaments.

The cooperativity of changes in F-actin becomes more clear when we consider the effect of F_{ab}, which binds only to one specific site in the actin monomer: $N \approx 5$ (Figure 5) suggests that its effect is transmitted to about four neighboring monomers. This long-range effect of F_{ab} on A_∞ supports the previously proposed explanation that the inhibitory effect on the activation of acto-S1 ATPase is due to the changes in the activating function of individual actin molecules through changes on adjacent, F_{ab}-occupied actins (*19*).

Direct evidence that nonlinear changes in A_∞ reflect not only local but also long-range changes in the actin filament is provided by the effect of copolymerization with EDC-actin, where the increase in A_∞ ($N \approx 7$, Figure 5) can be due only to the transfer of changes from the unlabeled EDC-actin to the labeled−untreated monomers within the same filament. Close pairs of carboxyl and lysine groups, which are required for EDC-induced cross-links in actin alone are distributed all over the monomer (*54*), and this could result in extensive modification. In particular, the EDC reaction with the carboxylic groups in the N terminus, which is responsible for cross-linking the heavy chain of myosin to actin in the rigor complex (*46, 55, 56*), could modify the myosin binding sites in this region, and the possibility of modification of the C terminus is indicated by cross-linking of the A1 light chain to this region (*37*). The similarity of the effects of copolymerization and S1 binding (Figures 5 and 9) suggests that these structural changes in EDC-actin have a long-range effect on the myosin binding sites in the untreated monomers.

The observed intermonomer cooperativity (Figure 5) likely results from the perturbation-induced changes at the C terminus. The C terminus has intra- and intermonomer effects on subdomain 2, which participates in intermonomer contacts along the actin helix (*54, 57−59*) and also interacts with the loop 262−274, which is supposed to stabilize interstrand contacts in the helix (*54, 60, 61*). Furthermore, proteolytic digestion and chemical modifications indicate that perturbations of this region of the actin monomer affect the structure and stability of the filament (*58, 62, 63*). The N terminus, also affected by the perturbations, does not seem to be directly involved in the intermonomer interactions (*64*).

Interpretation of Changes in A_∞ in Terms of Models of Molecular Motions. The increase in the normalized final anisotropy A_∞ (decrease in the amplitude of decay) upon perturbation of actin structure was analyzed in terms of two alternative models of rotational motions: intrafilament torsional twist and wobble-in-cone (Figure 7). According to the model of torsional twist, which attributes a change in A_∞ to a change in the orientation of the probe (*16, 30*), the observed increase in A_∞ indicates a rotation of the dye-binding site and/or the C terminus toward the filament axis by 15−20° (Table 2). On the other hand, the wobble-in-cone model interpreted the increase in A_∞ as a restriction of the angular amplitude of motions in actin. Since both torsional twist and wobble-in-cone fit the data equally well (Tables 1 and 2; Figure 7), we cannot exclude either model. Despite this ambiguity, the TPA data consistently imply that the perturbations induce allosteric and cooperative changes in the structure of the C-terminal region of actin. Previous interpretations of changes at the C terminus upon S1 binding from EPR and fluorescence data indicated a change in the environment of the probe (*8, 9, 13, 14*) or an increase of the radial coordinate of Cys 374 (*65, 66*).

Interpretation of Changes in the Time Constant Φ in Terms of Models of Molecular Motions. Early work on actin filaments suggested that its functional properties could be related to dynamic transformations of the intermonomer bonds (*67*), which led to numerous attempts to measure the rigidity of actin filaments (*7, 11, 12, 16, 68, 69*). The present work shows that perturbations of functional properties of actin change the rates of its rotational motions, i.e., the dynamics of the whole filament. Since we eliminated rigid-body rotations as a plausible explanation (Figure 7), the most likely interpretation is a change in the torsional rigidity of the filaments. The decrease of Φ upon copolymerization suggests a 3-fold decrease in the torsional rigidity C of the filament (eq 8; Table 2). However, the interpretation of the changes in the time constant Φ upon binding of S1 and F_{ab} requires consideration of changes not only in the torsional rigidity but also in the radius of the filament a (eq 8). The 4-fold increase in Φ upon binding of S1 (Table 2) is only half as much as expected from an increase in the filament radius a from 45 to 130 Å (a^2 increases by 8.3). Similarly, if we assume that the 50 kDa F_{ab} is the same size as an actin monomer, then the observed 2-fold increase in the time constant Φ (Table 2) is only half that due to the increased filament radius. Therefore, either (a) the assumed increases in a are overestimates or (b) binding of either S1 or F_{ab} decreases C by a factor of 2, i.e., decreases the torsional rigidity of the actin filament. A decrease in actin rigidity upon S1 binding has been previously concluded from electron and optical microscope studies (*11, 12*), but these measurements involved only filament bending, which is too slow to be detected on the time scale of the TPA experiment.

The torsional rigidity of actin filaments has recently been estimated from the rotational amplitude of a large polystyrene bead attached to actin (*70, 71*), but the obtained rigidity was about 50 times higher than that obtained from our TPA measurements (*16*). The simplest explanation for this discrepancy is that the bead, which slows down the rate of actin filament twisting motion by about 3 orders of magnitude, also decreases the amplitude of this motion, thus overestimating the torsional rigidity. It is also likely that actin dynamics covers a large time range, so it is not

surprising that the TPA technique, which detects motions in the microsecond-to-millisecond time range, reflects different molecular properties from video microscopy, which is sensitive to the millisecond-to-second time range. In any case, in the present study, we report that the microsecond motions detected by TPA are sensitive to functionally significant allosteric perturbations of actin.

Relationship between the Changes in TPA and Functional Interactions of Actin. Comparison of the results presented in this and previously published papers shows that the spectroscopic and functional changes were observed in a similar range of perturbations: the increase of $[F_{ab}(1-7)]/[A]$ to 0.45 and fraction of EDC-actin to 0.3, which resulted in maximum change in A_∞ (Figure 5), also resulted in ~50% inhibition of the activation of S1 ATPase (*19*) and the *in vitro* motility (Figure 6). Similar structural effects of F_{ab} and EDC-actin to the effects of rigor-bound S1 suggest that these functional changes are caused by transformation of actin to a form resembling a state in the rigor complex with myosin heads. The possibility that changes induced by rigor-bound heads may have inhibitory effect on actin motility is supported by our former studies, where we examined *in vitro* motility of acto-S1 complexes containing increasing amounts of S1 and NEM-modified S1 covalently cross-linked to actin by the bifunctional reagent disuccinimidyl suberate (DSS) (*23*). The inhibition of movement of ~50% of filaments required a higher fraction of monomers with bound S1 ($[S1]/[A] \geq 0.5$) than EDC-actin (≥ 0.3), and this difference in the inhibitory action of the two perturbations shows a remarkable correlation with the difference in the effectiveness in changing A_∞ (Figure 5). The proposed inhibitory role of structural changes similar to the changes induced by rigor-bound heads is not inconsistent with the presence of 20−30% heads bound to actin in the rigor-like conformation (*72*) in actively contracting muscle. This corresponds to a molar ratio of heads to actin of ~0.06−0.09 and is too low to affect the *in vitro* motility or induce significant structural changes in actin; these rigor heads could be involved in the mechanism of activation of the thin filament (*73*). The proposed transition of actin to a form resembling a myosin-bound rigor complex could affect the regions of electrostatic and hydrophobic interaction with myosin and, consequently, affect some steps in the actomyosin ATPase cycle. If structural transitions within actin are important for cyclic interaction with myosin, then the stabilization of one of actin's intermediate structure (e.g. proposed here structure that exists in rigor) should inhibit function of the actomyosin complex. This possibility of coupling structural changes in actin to the functional effects via the changes in the ATPase cycle has been recently proposed on the basis of biochemical studies on yeast actin mutants (*4*, *5*). The structural transitions in actin could also have implications for the mechanism of cooperative regulation of actin's functional state by a variety of actin binding proteins in muscle and nonmuscle cells.

On the other hand, the changes in A_∞ only partly overlap with the changes in motility (Figure 6), and therefore they cannot provide a complete explanation of the functional effects. Since actin is internally mobile in the time range from nanoseconds to milliseconds and in each range the motions are affected by interaction with myosin, some of the molecular motions that are required for motility may occur on a time scale not detected by TPA (microseconds). It is also likely that the mechanism of motility depends on structural changes that are not detected at the C terminus and that not every detected structural change has a functional effect. For example, we have shown that binding of gelsolin significantly affects A_∞ (*17*) but the actin−gelsolin filaments are motile in the *in vitro* motility assay as the filaments without gelsolin. The understanding of structure−function relationships in actin requires further examination of the effects of functional perturbations at wider time scale and detected by a probes located in different sites.

CONCLUSIONS

1. S1 binding induces cooperative changes in the microsecond rotational dynamics of actin, which reflect connectivity of structural changes within the actin monomer and filament.
2. Allosteric structural changes in the actin monomer and filament induced by $F_{ab}(1-7)$ and EDC-actin mimic the effect of S1 binding.
3. The correlation of these spectroscopically detected structural changes with function suggests that the actomyosin interaction can be inhibited by stabilization of actin in one of its structural intermediates.

ACKNOWLEDGMENT

We thank Dr. E. Reisler for generously providing the antibody fragment $F_{ab}(1-7)$, E. Howard for adapting the linear lattice model to analysis of our data, and R. L. H. Bennett and N. Cornea for excellent technical assistance.

REFERENCES

1. Cook, R. K., Blake, W. T., & Rubenstein, P. A. (1992) *J. Biol. Chem. 267*, 9430−9436.
2. Cook, R. K., Root, D., Miller, C., Reisler, E., & Rubenstein, P. A. (1993) *J. Biol. Chem. 268*, 2410−2415.
3. Miller, C. J., & Reisler, E. (1995) *Biochemistry 34*, 2694−2700.
4. Miller, C. J., Doyle, T. C., Bobkova, E., Botstein, D., & Reisler, E. (1996a) *Biochemistry 35*, 3670−3676.
5. Miller, C. J., Wong, W. W., Bobkova, E., Rubenstein, P. A., & Reisler, E. (1996b) *Biochemistry 35*, 16557−16565.
6. Schwyter, D. H., Kron, S. J., Toyoshima, Y. Y., Spudich, J. A., & Reisler, E. (1990) *J. Cell Biol. 111*, 465−470.
7. Yanagida, T., & Oosawa, F. (1978) *J. Mol. Biol. 126*, 507−524.
8. Kouyama, T., & Mihashi, K. (1980) *Eur. J. Biochem. 105*, 29−287.
9. Kouyama, T., & Mihashi, K. (1981) *Eur. J. Biochem. 114*, 33−38.
10. Miki, M., Wahl, P., & Auchet, J-C. (1982) *Biochemistry 21*, 3661−3665.
11. Takebayashi, T., Morita, Y., & Oosawa, F. (1977) *Biochim. Biophys. Acta 492*, 357−363.
12. Yanagida, T., Nakase, M., Nishiyama, K., & Oosawa, F. (1984) *Nature 307*, 58−60.
13. Thomas, D. D., Seidel, J. C., & Gergely, J. (1979) *J. Mol. Biol. 132*, 257−273.
14. Mossakowska, M., Belagyi, J., & Strzelecka-Golaszewska, H. (1988) *Eur. J. Biochem. 175*, 557−564.
15. Ostap, M., & Thomas, D. D. (1991) *Biophys. J. 59*, 1235−1241.
16. Prochniewicz, E., Zhang, Q., Howard, E., & Thomas, D. D. (1996a) *J. Mol. Biol. 255*, 446−457.
17. Prochniewicz, E., Zhang, Q., Janmey, P. A., & Thomas, D. D. (1996b) *J. Mol. Biol. 260*, 756−766.
18. Miller, L., Kalnoski, M., Yunossi, Z., Bulinski, J. C., & Reisler, E. (1987) *Biochemistry 26*, 6064−6070.

19. DasGupta, G., & Reisler, E. (1992) *Biochemistry 31*, 1836−1841.
20. Brenner, B., Kraft, T., DasGupta, G., & Reisler, E. (1996) *Biophys. J. 70*, 48−56.
21. Rayment, I., Holden, H. M., Whittaker, M., Yohn, C. B., Lorenz, M., Holmes, K. C., & Milligan, R. A. (1993) *Science 261*, 58−64.
22. Prochniewicz, E., & Yanagida, T. (1990) *J. Mol. Biol. 216*, 761−772.
23. Prochniewicz, E., Katayama, E., Yanagida, T., & Thomas, D. D. (1993) *Biophys. J. 65*, 113−123.
24. Honda, H., Kitano, Y., Hatori, K., & Matsuno, K. (1996) *FEBS Lett. 383*, 55−58.
25. Weeds, A. G., & Pope, B. (1977) *J. Mol. Biol. 111*, 129−157.
26. Bradford, M. M. (1976) *Anal. Biochem. 72*, 248−254.
27. Eads, T. M., & Thomas, D. D. (1984) *J. Mol. Biol. 179*, 55−81.
28. Ludescher, R. D., & Thomas, D. D. (1988) *Biochemistry 27*, 3343−3351.
29. Kinoshita, K., Kawato, S., & Ikegami, A. (1977) *Biophys. J. 20*, 289−305.
30. Schurr, J. M. (1984) *Chem. Phys. 84*, 71−96.
31. Ando, T., & Scales, D. (1985) *J. Biol. Chem. 260*, 2321−2327.
32. White, H. D., & Taylor, E. W. (1976) *Biochemistry 15*, 5818−5826.
33. McGhee, J. D., & von Hippel, P. H. (1974) *J. Mol. Biol. 86*, 469−489.
34. Uyeda, T. Q., Kron, S. J., & Spudich, J. (1990) *J. Mol. Biol. 214*, 699−710.
35. Milligan, R. A., & Flicker, P. F. (1987) *J. Cell Biol. 105*, 29−39.
36. Duong, A. M., & Reisler, E. (1994) in *Actin: Biophysics, Biochemistry, and Cell Biology* (Estes, J. E., & Higgins, P. J., Eds.) pp 59−70, Plenum Press, New York.
37. Sutoh, K. (1982) *Biochemistry 21*, 3654−3661.
38. Trayer, I. P., Trayer, H. R., & Levine, B. A. (1987) *Eur. J. Biochem. 164*, 259−266.
39. Kim, E., Miller, C., Motoki, M., Seguro, K., Muhlrad, A., & Reisler, E. (1996) *Biophys. J. 70*, 1439−1446.
40. Chen, T., Haigentz, M., Jr., & Reisler, E. (1992) *Biochemistry 31*, 2941−2946.
41. Miki, M., DosRemedios, C., & Barden, J. (1987) *Eur. J. Biochem. 168*, 339−345.
42. Moraczewska, J., Strzelecka-Golaszewska, H., Moens, P. D. J., & DosRemedios, C. G. (1996). *Biochem. J. 317*, 605−611.
43. Crosbie, R. H., Miller, C., Cheung, P., Goodnight, T., Muhlrad, A., & Reisler, E. (1994) *Biophys. J. 67*, 1957−1964.
44. Kim, E., Motoki, M., Seguro, K., Muhlrad, A., & Reisler, E. (1995) *Biophys. J. 69*, 2024−2032.
45. Kuznetsova, I., Antropova, O., Turoverov, K., & Khaitlina, S. (1996) *FEBS Lett. 383*, 105−108.
46. Mornet, D., Bertrand, R., Pantel, P., Audemard, E., & Kassab, R. (1981) *Nature 292*, 301−306.
47. Tawada, K., Wahl, P., & Auchet, J-C. (1978) *Eur. J. Biochem. 88*, 411−419.
48. Ng, C., & Ludescher, R. D. (1994) *Biochemistry 33*, 9098−9104.
49. Orlova, A., & Egelman, E. H. (1997) *J. Mol. Biol. 265*, 469−474.
50. Miki, M., Kouyama, T., & Mihashi, K. (1976) *FEBS Lett. 66*, 98−101.
51. Ando, T., & Asai, H. (1979) *J. Mol.Biol. 129*, 265−277.
52. Kouyama, T., & Mihashi, K. (1979) *Eur. J. Biochem. 105*, 279−287.
53. Kurzawa, S. E., & Geeves, M. A. (1996) *J. Muscle Res. Cell Motil. 17*, 669−676.
54. Holmes, K., Popp, D., Gebhard, W., & Kabsch, W. (1990) *Nature 347*, 44−49.
55. Elzinga, M. (1987) in *Methods in Protein Sequence Analysis* (Walsh, V. E., Ed.) pp 615−623, Humana Press, Clifton, NJ.
56. Bertrand, R., Chaussepied, P., Audemard, E., & Kassab, R. (1989) *Eur. J. Biochem. 181*, 747−754.
57. Orlova, A., & Egelman, E. H. (1993) *J. Mol. Biol. 232*, 334−341.
58. Orlova, A., & Egelman, E. H. (1995) *J. Mol. Biol. 245*, 582−597.
59. Kim, E., & Reisler, E. (1996) *Biophys. J. 71*, 1941−1919.
60. Chen, X., Cook, R. K., & Rubenstein, P. A. (1993) *J. Cell. Biol. 123*, 1185−1195.
61. Feng, L., Kim, E., Lee, W., Miller, C., Kuang, B., Reisler, E., & Rubenstein, P. (1997) *J. Biol.Chem. 272*, 16829−16837.
62. O'Donoghue, S., Miki, M., & dos Remedios, C. G. (1992) *Arch. Biochem. Biophys. 293*, 110−116.
63. Mossakowska, M., Moraczewska, J., Khaitlina, S., & Strzelecka-Golaszewska, H. (1993) *Biochem. J. 289*, 897−902.
64. DasGupta, G., White, J., Phillips, M., Bulinski, J. C., & Reisler, E. (1990) *Biochemistry 29*, 3319−3324.
65. Kasprzak, A., Takashi, R., & Morales, M. (1988) *Biochemistry 27*, 4512−4522.
66. Moens, P. D. J., & Dos Remedios, C. G. (1997) *Biophys. J. 72*, A239.
67. Oosawa, F., & Kasai, M. (1971) in *Subunits in Biological Systems, Part A* (Timasheff, Ed.) pp 261−322, Dekker, New York.
68. Isambert, H., Venier, P., Maggs, A. C., Fattoum, A., Kassab, R., Pantaloni, D., & Carlier, M-F. (1995) *J. Biol. Chem. 270*, 11437−11444.
69. Yoshimura, H., Nishio, T., & Mihashi, K. (1984) *J. Mol. Biol. 179*, 453−467.
70. Yasuda, R., Miyata, H., & Kinosita, K. (1966) *J. Mol. Biol. 263*, 227−236.
71. Tsuda, Y., Yasutake, H., Ishijima, A., & Yanagida, T. (1996) *Proc. Natl. Acad. Sci. U.S.A. 93*, 12937−12942.
72. Ostap, M. E., Barnett, V. A., & Thomas, D. D. (1995) *Biophys. J. 69*, 177−188.
73. Vibert, P., Craig, R., & Lehman, W. (1997) *J. Mol. Biol. 266*, 8−14.

BI971201R